Design and Dynamic Model of A Novel Powered Above Knee Prosthesis

Mucahit Ege
Biomedical Device Technology
Istanbul Gedik University
Istanbul, Turkey
mucahit.ege@gedik.edu.tr

Serdar Kucuk
Biomedical Engineering
Kocaeli University
Kocaeli, Turkey
skucuk@kocaeli.edu.tr

***Abstract*— Nowadays, fully active lower limb prostheses are very important for amputees to have comfort, aesthetic mobility and the ideal adaptation to daily life. However, active joint control is very difficult because of changing floor conditions, and it is essential to obtain a dynamic model of prostheses for system control. In this study, the design and dynamic model of a new above-knee prosthesis are presented. Firstly, the model design of the prosthesis was proposed by using Solidworks software environment and then kinematic and dynamic model was obtained as mathematical by using both Lagrange-Euler and also Newton-Euler method. The accuracy of the results has been proved with the same results obtained by both methods. MATLAB and Scientific Notebook software were used for those calculations. The torque equations required were obtained to perform joint movements with the dynamic model calculations and a simulation was performed to demonstrate the torques required for a gait cycle. Torque equations obtained were used for system control, motors selection and optimization in other studies.**

Keywords—Powered above knee prosthesis, prosthesis, kinematic model, dynamic model, Lagrange-Euler method, Newton-Euler method, robotic design, active prosthesis, robotic prosthesis, robotic trajectory

I. INTRODUCTION

The American Amputee Coalition reports that there are approximately 185,000 new lower extremity amputations each year, nearly 2 million people living with limb loss and adds that amputee population will more than double by the year 2050 just within the United States [1]. Therefore, prostheses are an important need for amputees to adapt to daily life.

There are three types of prosthesis; passive [2, 3], semi-active [4-6] and active prosthesis [7–10]. Nowadays, widely used prostheses are passive and semi-active prostheses which are simple devices that allow amputees to perform basic walking functions and cannot provide the need for amputees. However, active prostheses provide the best walking performance to amputees when compared with other conventional types. More complex and comfortably prostheses with multi-axes ability are needed to provide natural walking and those systems are a kind of robotic manipulators. Today, researches on active lower limb prostheses are still in experimental stage [11-14]. Because more complex systems bring some difficulties such as more weight, complex control algorithms, and energy consumption. However, firstly kinematic and dynamic model have to be obtained accurately to control an active robotic prosthesis.

The forward kinematics of the robot are concerned with the relationship between the positions, velocities, and accelerations of the robot links [15]. The solution of kinematic problems is generally carried out in three-dimensional cartesian space. Exponential and Pieper-Roth methods can be used for kinematic solutions [16]. However, the Denavit-Hartenberg (D-H) method is generally preferred [17]. In order to understand how a robotic system moves under certain conditions, it is necessary to have knowledge about the dynamics of this system, including values such as force, inertia and energy [18].

Sha and his friends presented dynamic analysis and optimization for the ankle joint prosthesis [19]. They proposed an ankle joint prosthesis which has the function of energy storage and release. They used ADAMS software for dynamic simulation and reported that the parameters were optimized and optimal spring stiffness was achieved.

Richter and his friends presented the development, modeling, parameter estimation and control of a robot capable of reproducing two degree-of-freedom hip motion in the sagittal plane to test prosthetic limbs. They reported that they used robot dynamic modeling for test machine and prosthesis successfully with leading a simulation model.

In this study, a new fully active above-knee prosthesis model, which has three axes movement capability was designed. Mechanism of the ankle, on both axes actuated with or without actuators, were patented [20]. Forward kinematic model and dynamic model were obtained respectively. The kinematic model was obtained by using the D-H method. A dynamic model was obtained both Lagrange-Euler method and also Newton-Euler method. It was aimed to get accurate results by comparing the results obtained with both two methods and torque values are obtained for each joint of the prosthesis. A simulation was carried out to demonstrate the torques required for a gait cycle. These values were used for system control, motor selection and optimization in our other studies.

II. METHOD AND MATERIAL

A. Model of Prosthesis

The above knee prosthesis designed has three joints which are at knee and ankle. Figure 2 demonstrates the design and

978-1-7281-2420-9/19/$31.00 ©2019 IEEE

geometric structure of the above-knee prosthesis. The ankle joint has two axes movement; they are plantar flexion-dorsal flexion and inversion-eversion. Each joint was actuated with a DC motor. Maxon DCX35L DC motor was used for each joint, but for reduction, Maxon GP42 gearhead with 16:1 reduction ratio was used both at the ankle joint for plantar-dorsal flexion and also at the knee joint for flexion-extension. At the same time, Maxon GP40 gearhead with a 15:1 reduction ratio was used at the ankle joint for eversion-inversion. Ball screws were used for transmission of rotational force from DC motors to knee and ankle joints to provide flexion-extension of the knee joint and plantar flexion-dorsal flexion of the ankle. These motors were placed to tibia region of the prosthesis. Eversion-inversion of the ankle joint was actuated with a motor placed in the foot.

We designed the above-knee prosthesis by using Solidworks software and manufactured it using PLA (Poly Lactic Acid) filament as material via a 3D printer. Figure 1 shows the designed and produced pictures of the prosthesis.

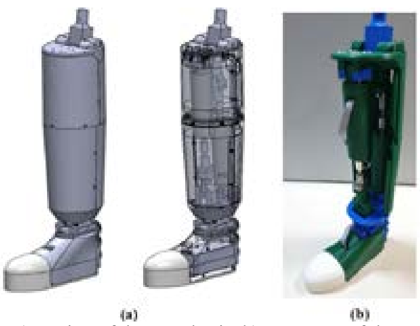

Figure 1. a) Design of the prosthesis, b) prototype of the prosthesis

PLA is a low-cost material and easily available. It has a low manufacturing cost easy to process according to the conventional manufacturing process by using the 3D printer. It is printed at lower temperatures than other 3D materials that provide energy efficiency. Additionally, it is lighter than conventional materials used for a prosthesis. PLA is an organic and biocompatible material, so toxic gases are not released during the manufacturing process and the surfaces which contact the human body does not have any harmful effect. That is why PLA was chosen as the material of the prototype.

B. Kinematic Model

The joints and links of the prosthesis were determined and coordinate systems were placed to each joint. It was shown in Figure 2.

D-H variables were determined according to the Figure 2 and were given in Table 1. $\alpha_{i-1}, a_{i-1}, d_i$ and θ_i are the distance from Z_i to Z_{i+1} measured along X_i, the angle from Z_i to Z_{i+1} measured about X_i, the distance from X_{i-1} to X_i measured along Z_i and the angle from X_{i-1} to X_i measured along Z_i respectively.

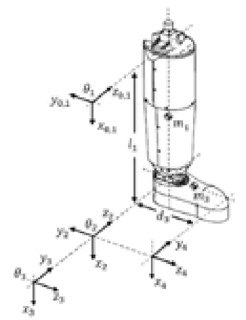

Figure 2. Prosthetic leg and coordinate systems

TABLE 1. D-H VARIABLES OF THE PROSTHESIS

i	α_{i-1}	a_{i-1}	d_i	θ_i
1	0	0	0	θ_1
2	0	l_1	0	θ_2
3	90	0	0	θ_3
4	0	0	d_3	0

The transformation matrices were calculated as follows by using the D-H variables obtained in Table 1.

$$ {}^0_4T = {}^0_1T\,{}^1_2T\,{}^2_3T\,{}^3_4T \quad (1)$$

Position and orientation of toe of the prosthesis were obtained as follows.

$$ {}^0_4T = \begin{bmatrix} r_{11} & r_{12} & r_{13} & p_x \\ r_{21} & r_{22} & r_{23} & p_y \\ r_{31} & r_{32} & r_{33} & p_z \\ 0 & 0 & 0 & 1 \end{bmatrix} \quad (2)$$

p_x, p_y, p_z and $r_{11}, r_{12}, r_{13}, r_{21}, r_{22}, r_{23}, r_{31}, r_{32}, r_{33}$ are the positions and orientations of end-point of prosthesis in cartesian space in equation (2).

C. Dynamic Model

The dynamic model was obtained both Lagrange-Euler method and also Newton-Euler method. Matlab and Scientific Notebook software were used for calculations and simulations.

The dynamic equations of the prosthesis can be expressed as equation (3).

$$\tau = D(\theta)\ddot{\theta} + C(\theta,\dot{\theta}) + H(\theta) + B(\dot{\theta}) \quad (3)$$

In the equation (3), D denotes the nxn mass matrix, C $nx1$ Coriolis and the centrifugal force vector, H $nx1$ gravity vector and B is the $nx1$ friction vector. In addition, τ, θ, $\dot{\theta}$ and $\ddot{\theta}$ indicate nx1 joint torques, their position, speed and acceleration, respectively.

1) Lagrange-Euler Method: In this chapter, the dynamic model of the prosthesis was calculated by using the Lagrange-Euler method. The position of the mass center of each link was given as the following vectors.

$$\Delta h_1 = \begin{bmatrix} \frac{l_1}{2} \\ 0 \\ 0 \\ 1 \end{bmatrix}, \Delta h_2 = \begin{bmatrix} 0 \\ -\frac{d_3}{2} \\ 0 \\ 1 \end{bmatrix}, \Delta h_3 = \begin{bmatrix} 0 \\ 0 \\ \frac{d_3}{2} \\ 1 \end{bmatrix} \quad (4)$$

h_i denotes the coordinates of the mass center of the i*th* link and was calculated as the equation (5).

$$h_i = {}_i^0T\Delta h_i \qquad i=1,2,3 \quad (5)$$

The inertia tensor (I_i) of the i*th* link relative to the main coordinate system was obtained as follows. I_{mi} denotes the inertia tensor of the mass center of the i*th* link.

$$I_i = {}_i^0RI_{mi}\,{}_i^0R^T \qquad i=1,2,3 \quad (6)$$

The linear Jacobian matrix (A_i) and the angular Jacobian matrix (B_i) of the i*th* joint were calculated as equation (7).

$$J_i = [A_i \quad B_i]^T \qquad i=1,2,3 \quad (7)$$

Mass matrix of the i*th* joint was calculated with equation (8).

$$D(\theta_i) = m_iA_i^TA_i + B_i^TI_iB_i \qquad i=1,2,3 \quad (8)$$

As a result, the total dynamic equation of the prosthetic leg was obtained as equation (9). This equation gives torque values of each joint.

$$\begin{bmatrix} \tau_1 \\ \tau_2 \\ \tau_3 \end{bmatrix} = \begin{bmatrix} D_{11} & D_{12} & D_{13} \\ D_{21} & D_{22} & D_{23} \\ 0 & 0 & D_{33} \end{bmatrix} \begin{bmatrix} \ddot\theta_1 \\ \ddot\theta_2 \\ \ddot\theta_3 \end{bmatrix} + \begin{bmatrix} C_1(\theta,\dot\theta) \\ C_2(\theta,\dot\theta) \\ C_3(\theta,\dot\theta) \end{bmatrix} + \begin{bmatrix} H_1(\theta) \\ H_2(\theta) \\ H_3(\theta) \end{bmatrix} \quad (9)$$

2) Newton Method: In this chapter, the dynamic model of the prosthesis was calculated by using the Newton-Euler method. Firstly, outward equations were obtained for Newton-Euler method. Angular velocity transmitted from one joint to another were calculated with equation (10).

$$^{i+1}\omega_{i+1} = {}_i^{i+1}R\,{}^i\omega_i + \dot\theta_{i+1}\,{}^{i+1}\hat{Z}_{i+1} \qquad i=0,1,2 \quad (10)$$

Angular acceleration transmitted from one joint to another were calculated with equation (11) where i=0, 1 and 2.

$$^{i+1}\dot\omega_{i+1} = {}_i^{i+1}R\,{}^i\dot\omega_i + \ddot\theta_{i+1}\,{}^{i+1}\hat{Z}_{i+1} + {}_i^{i+1}R\,{}^i\omega_i x\dot\theta_{i+1}\,{}^{i+1}\hat{Z}_{i+1} \quad (11)$$

The linear acceleration of the i*th* joint was obtained with equation (12).

$$^{i+1}\dot v_{i+1} = {}_i^{i+1}R\left({}^i\dot\omega_i x\,{}^iP_{i+1} + {}^i\omega_i x\left({}^i\dot\omega_i x\,{}^iP_{i+1}\right) + {}^i\dot v_i\right) \qquad i=0,1,2 \quad (12)$$

The linear acceleration of the mass center of the i*th* joint was obtained using equation (13) where i=0, 1 and 2.

$$^{i+1}\dot v_{C_{i+1}} = {}^{i+1}\dot\omega_{i+1} x\,{}^{i+1}P_{C_{i+1}} + {}^{i+1}\omega_{i+1} x({}^{i+1}\omega_{i+1} x\,{}^{i+1}P_{C_{i+1}}) + {}^{i+1}\dot v_{i+1} \quad (13)$$

Force vector of the i*th* joint was calculated with equation (14).

$$^{i+1}F_{i+1} = m_{i+1}\,{}^{i+1}\dot v_{C_{i+1}} \qquad i=0,1,2 \quad (14)$$

And moment vector of the i*th* joint was obtained using equation (15).

$$^{i+1}N_{i+1} = {}^{C_{i+1}}I_{i+1}\,{}^{i+1}\dot\omega_{i+1} + {}^{i+1}\omega_{i+1} x({}^{C_{i+1}}I_{i+1}\,{}^{i+1}\omega_{i+1}) \qquad i=0,1,2 \quad (15)$$

Then, inward equations were obtained for Newton-Euler method. The force on the i*th* joint was calculated with equation (16).

$$^if_i = {}_{i+1}^{i}R\,{}^{i+1}f_{i+1} + {}^iF_i \qquad i=0,1,2 \quad (16)$$

The torque on the i*th* joint was obtained using equation (17) where i=0, 1 and 2.

$$^in_i = {}^iN_i + {}_{i+1}^{i}R\,{}^{i+1}n_{i+1} + {}^iP_{C_i} x\,{}^iF_i + {}^iP_{i+1} x\,{}_{i+1}^{i}R\,{}^{i+1}f_{i+1} \quad (17)$$

Same torque equations were obtained with both methods and the accuracy of dynamic equations is proved.

D. Trajectory of System

Third order or higher degrees of polynomials are used for trajectory planning of robotic applications. In this project, end-effector is toe and third order polynomial was used for trajectory planning [15].

The initial position of the end function at t is $\theta(0) = \theta_1$ and the target position at t_f is $\theta(t_f) = \theta_f$.Initial and final velocities $\dot\theta(0) = 0$ and $\dot\theta(t_f) = 0$ [15].

Equations (18), (21) and (24) were used for the positions depending on the angles θ_1, θ_2 and θ_3 of the joints, respectively. Equations (19), (22) and (25) were obtained for getting the velocities of the joints by taking the first derivative of these equations. By taking the second derivative, Equation (20), (23) and (26), which are acceleration equations, were obtained.

$$\theta_1(t) = s_0^1 + s_1^1t + s_2^1t^2 + s_3^1t^3 \quad (18)$$

$$\dot\theta_1(t) = s_1^1 + 2s_2^1t + 3s_3^1t^2 \quad (19)$$

$$\ddot\theta_1(t) = 2s_2^1 + 6s_3^1t \quad (20)$$

$$\theta_2(t) = s_0^2 + s_1^2t + s_2^2t^2 + s_3^2t^3 \quad (21)$$

$$\dot\theta_2(t) = s_1^2 + 2s_2^2t + 3s_3^2t^2 \quad (22)$$

$$\ddot\theta_2(t) = 2s_2^2 + 6s_3^2t \quad (23)$$

$$\theta_3(t) = s_0^3 + s_1^3t + s_2^3t^2 + s_3^3t^3 \quad (24)$$

$$\dot\theta_3(t) = s_1^3 + 2s_2^3t + 3s_3^3t^2 \quad (25)$$

$$\ddot\theta_3(t) = 2s_2^3 + 6s_3^3t \quad (26)$$

E. RESULTS AND DISCUSSION

In order to see the trajectory of the prosthesis in Cartesian space, it was obtained using equation (2) for a gait cycle and this trajectory was illustrated in Figure (3).

Figure 4 presents the positions, velocities and accelerations of the joints depending on the equation (18)-(26) for a gait cycle. A gait cycle was assumed of 2.5 second.

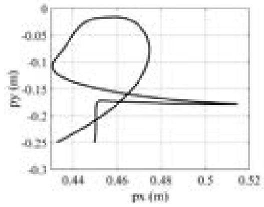

Figure 3. Toe Cartesian trajectory of the prosthesis

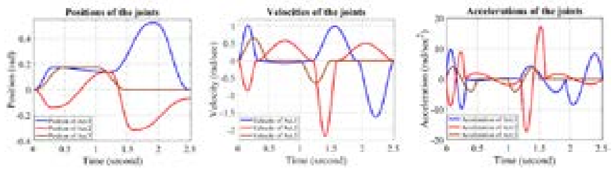

Figure 4. Position, velocity and acceleration of all joints of the prosthesis for a gait cycle

l_1, d_3 and m_1, m_3 are the dynamic model simulation parameters and illustrate the link lengths and masses. Simulation parameters were determined as; $\mathrm{l}_1 = 0.45\mathrm{m}$, $\mathrm{d}_3 = 0.25\mathrm{m}$, $\mathrm{m}_1 = 1.74\mathrm{kg}$, $\mathrm{m}_3 = 1.34\mathrm{kg}$. It was simulated without the user's weight being loaded on the prosthesis and obtained torques shown in Figure 5.

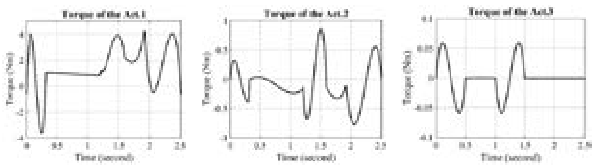

Figure 5. Torques on each joint for a gait cycle

Dynamic model results gave us the torque equations of the joints. We carry out a simulation to see the results and we obtained maximum torques as 4.2Nm at the knee, 0.8Nm at the ankle for plantar-dorsal flexion and 0.06Nm at the ankle for eversion-inversion. Knee torque results are greater than other axes because of having l_1 of weight. Masses in axis 2 and 3 are the same, but the torques are different since the load distribution on the axes is different. These values are sufficient for the swing phase of a natural walking, but it was not tested for the stance phase yet.

III. CONCLUSION

In this study, design and dynamic model of a powered above knee prosthesis were presented. An active above knee prosthesis with three axes that can move at one axis in the knee and at two axes in the ankle was designed to obtain the ability to walk closest to the movements of a healthy person. Firstly, design details were presented of the prosthesis and kinematic model was obtained by determining the D-H parameters on the model. Then, the dynamic model was obtained both Lagrange-Euler method and also Newton-Euler method. In this way, we proved the results' accuracy by comparing the results obtained with both two methods. Dynamic model results gave us the torque equations of the joints. These equations were verified with a simulation for a gait cycle and it was seen the results in the desired range.

ACKNOWLEDGMENT

This project is supported by The Scientific and Technological Research Council of Turkey (TÜBİTAK-3001, Project Number: 116M322).

REFERENCES

[1] Ziegler-Graham, K., MacKenzie, E. J., Ephraim, P. L., Travison, T. G., & Brookmeyer, R. (2008). Estimating the prevalence of limb loss in the United States: 2005 to 2050. *Archives of physical medicine and rehabilitation*, 89(3), 422-429.

[2] R. Unal, R. Carloni, S. M. Behrens, E. E. G. Hekman, S. Stramigioli, and H. F. J. M. Koopman, "Towards a fully passive transfemoral prosthesis for normal walking," *Proc. IEEE RAS EMBS Int. Conf. Biomed. Robot. Biomechatronics*, pp. 1949–1954, 2012.

[3] S. M. Behrens, R. Unal, E. E. G. Hekman, R. Carloni, S. Stramigioli, and H. Koopman, "Design of a fully-passive transfemoral prosthesis prototype," in *2011 Annual International Conference of the IEEE Engineering in Medicine and Biology Society*, 2011, pp. 591–594.

[4] M. V. Pillai, H. Kazerooni, and A. Hurwich, "Design of a semi-active knee-ankle prosthesis," *Proc. - IEEE Int. Conf. Robot. Autom.*, pp. 5293–5300, 2011.

[5] M. I. Awad *et al.*, "Towards a Smart Semi-Active Prosthetic Leg: Preliminary Assessment and Testing," *IFAC-PapersOnLine*, vol. 49, no. 21, pp. 170–176, 2016.

[6] B. G. A. Lambrecht and H. Kazerooni, "Design of a semi-active knee prosthesis," *Proc. - IEEE Int. Conf. Robot. Autom.*, pp. 639–645, 2009.

[7] W. Carlos, S. Júnior, M. Aurélio, V. De Oliveira, and J.-J. Bonvent, "Conception, design and development of a low-cost intelligent prosthesis for one-sided transfemoral amputees."

[8] A. O. Kapti and M. S. Yucenur, "Design and control of an active artificial knee joint," *Mech. Mach. Theory*, vol. 41, no. 12, pp. 1477–1485, 2006.

[9] A. S. Kulkarni and S. M. Kulkarni, "Robotic Leg Prosthesis," *2017 Int. Conf. Adv. Mechatronics, Intell. Manuf. Ind. Autom.*, pp. 97–103, 2017.

[10] A. H. Shultz, B. E. Lawson, and M. Goldfarb, "Running with a powered knee and ankle prosthesis," *IEEE Trans. Neural Syst. Rehabil. Eng.*, vol. 23, no. 3, pp. 403–412, 2015.

[11] S. K. Au, H. Herr, J. Weber, and E. C. Martinez-Villalpando, "Powered ankle-foot prosthesis for the improvement of amputee ambulation," *Annu. Int. Conf. IEEE Eng. Med. Biol. - Proc.*, pp. 3020–3026, 2007.

[12] J. D. Ventura, G. K. Klute, and R. R. Neptune, "The effects of prosthetic ankle dorsiflexion and energy return on below-knee amputee leg loading," *Clin. Biomech.*, vol. 26, no. 3, pp. 298–303, 2011.

[13] E. H. Sinitski, A. H. Hansen, and J. M. Wilken, "Biomechanics of the ankle–foot system during stair ambulation: Implications for design of advanced ankle–foot prostheses," *J. Biomech.*, vol. 45, no. 3, pp. 588–594, 2012.

[14] H. A. Varol, F. Sup, and M. Goldfarb, "Powered sit-to-stand and assistive stand-to-sit framework for a powered transfemoral prosthesis," *2009 IEEE Int. Conf. Rehabil. Robot. ICORR 2009*, pp. 645–651, 2009.

[15] Z. Bingül and S. Küçük, *Robot kinematiği*. Birsen Yayınevi, 2009.

[16] M. K. Özgören, "Application of exponential rotation matrices to the kinematic analysis of manipulators," in *Proceedings Seventh World Congress on the Theory of Machines and Mechanisms*, 1987, pp. 1187–1190.

[17] R. S. Hartenberg and J. Denavit, "A kinematic notation for lower pair mechanisms based on matrices," *J. Appl. Mech.*, vol. 77, no. 2, pp. 215–221, 1955.

[18] Z. Bingül and S. Küçük, *Robot dinamiği ve kontrolü*. Birsen Yayınevi, 2008.

[19] H. Sha *et al.*, "Dynamic analysis and optimization for the ankle joint prosthesis," in *2015 IEEE International Conference on Rehabilitation Robotics (ICORR)*, 2015, pp. 283–288.

[20] M. Ege and S. Küçük, "Protez bacaklar için Modüler Ayak Bileği Eklem Mekanizması", Türk Patent ve Marka Enstitüsü, Patent No: 201723575.